Inhibiting Shear Instability Induced by Large Amplitude Internal Solitary Waves in Two-Layer Flows with a Free Surface

By Ricardo Barros and Wooyoung Choi

We consider a strongly nonlinear long wave model for large amplitude internal waves in two-layer flows with the top free surface. It is shown that the model suffers from the Kelvin–Helmholtz (KH) instability so that any given shear (even if arbitrarily small) between the layers makes short waves unstable. Because a jump in tangential velocity is induced when the interface is deformed, the applicability of the model to describe the dynamics of internal waves is expected to remain rather limited. To overcome this major difficulty, the model is written in terms of the horizontal velocities at the bottom and the interface, instead of the depth-averaged velocities, which makes the system linearly stable for perturbations of arbitrary wavelengths as long as the shear does not exceed a certain critical value.

1. Introduction

Large amplitude oceanic internal waves is a ubiquitous phenomenon that despite being known for centuries, has only been recently the subject of scientific studies. They manifest on the surface of the sea by long isolated stripes of highly agitated features that are defined as audibly breaking waves and white

Address for correspondence: W. Choi, Department of Mathematical Sciences and Center for Applied Statistics, New Jersey Institute of Technology, Newark, NJ 07102-1982, USA; e-mail: wychoi@njit.edu

STUDIES IN APPLIED MATHEMATICS 122:325–346

water. These waves have amplitudes that can exceed 100 m, wavelengths of order of km, and move with speeds of order of 1 m/s.

To understand this phenomenon, the Euler equations (or even the Navier–Stokes equations) for density-stratified flows should be solved; however, these equations are not easily amenable to analytical investigations and, even today, numerical simulations for models based on the Euler equations are computationally too expensive. For these reasons, simple analytical models describing some of the essential physics found in these full hydrodynamic equations are still desirable. Long wave models of Miyata [1] and Choi and Camassa [2] for a two-layer system under the rigid-lid assumption, combining both relative simplicity and full nonlinearity, have been developed and have been found to be a good approximation to the Euler equations even for the strongly nonlinear regime as long as its traveling wave solutions are concerned [3]. The model also shows excellent agreement with laboratory experiments of Grue et al. [4] and Michallet and Barthelemy [5] for the shallow and deep water configurations, respectively.

On the other hand, the presence of a top free surface might have some important effects that cannot be captured by the rigid-lid model. One example is the generalized solitary waves that can only exist for the free-surface case (see [6, 7]). In this case, internal solitary waves with multi-humped profiles have been observed by Barros and Gavrilyuk [8]. Also, on the hyperbolicity of the two-layer shallow water equations, distinct features between the two configurations can be found [9]. These indicate that the free-surface effects could be worth to explore.

Strongly nonlinear models describing large amplitude waves in a two-layer fluid with the top free surface were first derived by Choi and Camassa [10] by using asymptotic analysis, and more recently by Barros, Gavrilyuk, and Teshukov [11] by using a variational approach. These two models agree and are a two-layer generalization of the Su–Gardner equations [12] (also referred to as the Green–Naghdi equations [13] in the literature). Liska, Margolin, and Wendroff [14] also derived a similar set of equations by assuming that the vertical velocity is a linear function of the vertical coordinate. Unfortunately, due to the complex form in which they are presented, the equations of Liska et al. [14] are not easily amenable to analytical investigations and are even difficult to compare with the set of equations to be used in this paper.

The one-dimensional version of the strongly nonlinear long wave model (see [10, 11]) is written in terms of the layer thicknesses h_i and the depth-averaged velocities $\bar{u}_i$ ($i = 1$ and 2 represent the lower and upper layers, respectively):

$$h_{1t} + (h_1\bar{u}_1)_x = 0,$$
$$h_{2t} + (h_2\bar{u}_2)_x = 0,$$

$$\bar{u}_{1t} + \bar{u}_1\bar{u}_{1x} + g(h_1 + \rho h_2)_x + \rho\left(-\frac{1}{2}G_2h_2^2 + \left(D_2^2h_1\right)h_2\right)_x = \frac{1}{3h_1}\left(h_1^3G_1\right)_x,$$
$$\bar{u}_{2t} + \bar{u}_2\bar{u}_{2x} + g(h_1 + h_2)_x = \frac{1}{3h_2}\left(h_3^2G_2\right)_x - \frac{1}{2h_2}\left(h_2^2\,D_2^2h_1\right)_x + \left(\frac{1}{2}h_2G_2 - D_2^2h_1\right)h_{1x}. \tag{1}$$

where g is the gravitational acceleration, ρ_i are the fluid densities with $\rho_2 < \rho_1$ for stable stratification, and the subscripts x and t represent partial differentiation with respect to space and time, respectively. We have also introduced the density ratio $\rho < 1$ defined by $\rho = \rho_2/\rho_1$, the second-order material derivative of h_1 with respect to the averaged velocity field $\bar{u}_2$ denoted here by $D_2^2h_1$, where $D_2 = \partial_t + \bar{u}_2\partial_x$, and the nonlinear dispersive terms G_i given by

$$G_i = \bar{u}_{ixt} + \bar{u}_i\bar{u}_{ixx} - \bar{u}_{ix}{}^2.$$

The system is endowed with a Hamiltonian structure and the momentum equations can be found as the Euler–Lagrange equations for an approximate Lagrangian to the Euler equations for two-layer flows with the free surface [11]. This same structure holds also for its traveling-wave solutions, which revealed in [8] as a valuable tool to characterize these solutions. In their paper, Barros and Gavrilyuk [8] have shown quite a rich diversity of solitary-wave solutions that is absent in the rigid-lid case. In particular, the multi-humped solitary-wave solutions exhibited there show the richness and complexity of the Hamiltonian system with two degrees of freedom describing traveling-wave solutions.

Unfortunately, a major difficulty is expected in solving numerically this model for the study of the propagation of solitary waves. Although no background shear is present when the interface is flat, a jump in tangential velocity, leading to a Kelvin–Helmholtz (KH) instability, is induced when the interface is deformed since the model was derived under the inviscid assumption, which requires only continuity of normal velocity. The same difficulty is present for the rigid-lid configuration, as pointed out by Jo and Choi [15]. In an attempt to overcome this difficulty, Jo and Choi [16] proposed the use of a low-pass filter to remove unstable short waves which enables one to simulate the propagation of a single solitary wave of large amplitude for a long time. The drawback of this approach is the difficulty of applying the same technique to general time-dependent problems.

A recent work by Choi, Barros, and Jo [17] addresses the problem with more promising results for a two-layer system bounded by rigid walls. Adopting the idea of Nguyen and Dias [18] for a weakly nonlinear model, Choi et al. [17] expressed the strongly nonlinear model in terms of the horizontal velocities at certain preferred vertical levels, instead of the depth-averaged velocities. Through local stability analysis under the assumption that the

velocity jump varies slowly in space, it was shown that the new form of the strongly nonlinear model changes the dispersion relation in a way that internal solitary waves become stable to perturbations of arbitrary wavelengths as long as their amplitudes do not exceed a certain critical value. In fact, this critical amplitude is found to be close enough to the maximum amplitude for a wide range of physical parameters, which opens the possibility of using the model for real applications in the strongly nonlinear regime.

In this paper, we will first show that our original strongly nonlinear model with the top free surface suffers from the KH instability. Then, following Choi et al. [17], we propose a strongly nonlinear model that is asymptotically equivalent to the original one, but has a different dispersive behavior for short waves. Compared with the rigid-lid model, the free-surface model given by (1) yields a much more complex dispersion relation due to the two extra degrees of freedom. It will be shown analytically that, by considering the velocities at the bottom and the interface, the dispersion relation is modified in a way that this KH instability is contained up to a certain critical shear between the layers.

2. Shear instability for the original strongly nonlinear model

By looking for solutions $(h_1, h_2, \bar{u}_1, \bar{u}_2) \sim \exp[i(kx - \omega t)]$ of the system of Equations (1) linearized about $\bar{u}_i = U_i$ and $h_i = H_i$, we obtain the following linear dispersion relation between ω and k:

$$\left[\left(1 + \frac{1}{3}k^2 H_1^2\right)(c - U_1)^2 - gH_1\right]\left[\left(1 + \frac{1}{3}k^2 H_2^2\right)(c - U_2)^2 - gH_2\right] + \rho H_1 H_2 \left[k^2\left(1 + \frac{1}{12}k^2 H_2^2\right)(c - U_2)^4 - g^2\right] = 0, \tag{2}$$

where k is the wave number, ω is the wave frequency, and $c = \omega/k$ is the wave speed. In (2), the horizontal velocities U_i induced by a slowly varying solitary wave are assumed to be locally constant. We will prove that, for any given shear between layers, there exists a critical wave number k_{cr} such that Equation (2) has complex roots for $k > k_{cr}$. This implies that the strongly nonlinear internal wave model (1) is always linearly unstable to short-wavelength perturbations. To prove this, we write Equation (2) in terms of nondimensional variables:

$$\bar{c} = \frac{c}{\sqrt{gH_1}}, \quad H = \frac{H_2}{H_1}, \quad K = kH_1, \quad F = \frac{U_2 - U_1}{\sqrt{gH_1}}, \tag{3}$$

and assume without loss of generality that $u_1/\sqrt{gH_1} = 1$ (by choosing a moving reference frame such this condition is met). Then, the dispersion relation becomes

$$a_0\bar{c}^4 + a_1\bar{c}^3 + a_2\bar{c}^2 + a_3\bar{c} + a_4 = 0, \tag{4}$$

where the coefficients are functions of ρ, H, F, and K (see Appendix A). We remark that the strongly nonlinear model under the rigid-lid approximation yields a quadratic equation for the wave speed c. In the free-surface case, as a consequence of the two extra degrees of freedom, the dispersion relation becomes a quadratic equation. For this equation, we seek relations involving these parameters for which Equation (4) has only real roots. Notice that the system is always linearly stable for $F = 0$ since the dispersion relation (2) reduces to a biquadratic form with four distinct real solutions (see [8]).

Several attempts have been made in the past to obtain conditions in terms of the literal coefficients of a polynomial, concerning a special root distribution (see [19] and references therein). Among them, Jury and Mansour [19] presented a series of algorithms involving characteristic expressions for a quartic equation, allowing a full characterization of the root distribution in a much more concise form than the one provided by previous approaches. Similar criteria involving only inner determinants were also obtained by Fuller [20]. Following this elegant exposition, when considering the inner determinants Δ_3, Δ_5, Δ_7:[1]

$$\Delta_7 = \begin{vmatrix} a_0 & a_1 & a_2 & a_3 & a_4 & 0 & 0 \\ 0 & a_0 & a_1 & a_2 & a_3 & a_4 & 0 \\ 0 & 0 & a_0 & a_1 & a_2 & a_3 & a_4 \\ 0 & 0 & 0 & 4a_0 & 3a_1 & 2a_2 & a_3 \\ 0 & 0 & 4a_0 & 3a_1 & 2a_2 & a_3 & 0 \\ 0 & 4a_0 & 3a_1 & 2a_2 & a_3 & 0 & 0 \\ 4a_0 & 3a_1 & 2a_2 & a_3 & 0 & 0 & 0 \end{vmatrix},$$

with Δ_3 and Δ_5 being defined as the determinants of the inner matrices with dimensions 3×3 and 5×5, respectively (as denoted by the two inner squares in the definition of Δ_7), we have the following result (see [20], p. 778):

THEOREM *1. Equation (4) with $a_0 > 0$ has its roots all real if and only if one of the two following sets of conditions holds:* (*a*) $\Delta_3 > 0$, $\Delta_5 > 0$, $\Delta_7 \geqslant 0$; (*b*) $\Delta_3 \geqslant 0$, $\Delta_5 = 0$, $\Delta_7 = 0$.

For this theorem to be valid, the highest-order coefficient a_0 in (4) must be positive. In our case, this requirement is always satisfied, as shown in Appendix A.

For prescribed values of ρ and H, thanks to the built-in function `RegionPlot` of MATHEMATICA 6.0, we can visualize the stable (shaded) and unstable

[1]Notice that Δ_7 is precisely the discriminant of the quartic Equation (4) and hereafter will be denoted by Δ.

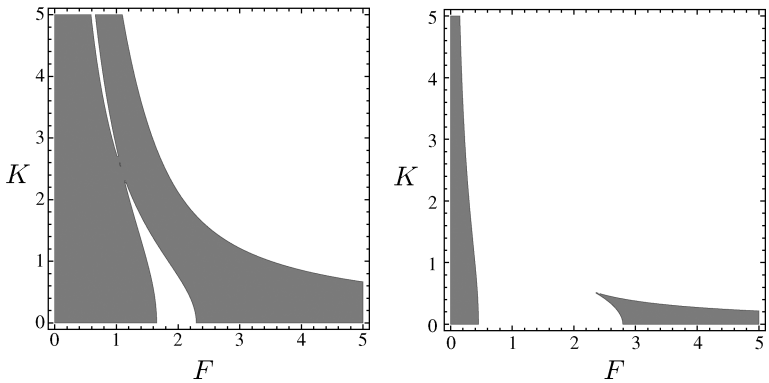

Figure 1. Shear instability of the original strongly nonlinear model (1) on the (F, K)-plane for different physical parameters: $\rho = 1/10$ (*left-hand side*) and $\rho = 9/10$ (*right-hand side*). In both cases, we have considered $H = 1$. In this figure, the shaded and unshaded regions represent the stable and unstable regions, respectively.

(unshaded) regions on the (F, K)-plane, as shown in Figure 1. For $H = 1$, a clear distinction between two different density ratios is displayed in this figure. For the case of a small density ratio on the left-hand side, we detect two ranges of the Froude number, for any given K, for which the system is stable. The same does not hold for large density ratios. We see on the right-hand side that, while two branches of stability persist for small values of K, one of the branches no longer exists when K exceeds a certain wave number. Are these observations made for $H = 1$ still valid for different values of H? Moreover, for fixed values of ρ and H, how can one predict which scenario applies? To answer these questions, we adopt a geometrical representation of the problem. Then, we will prove that the set of conditions in Theorem 1 can be reduced to $\Delta \geqslant 0$ or, equivalently, $\Delta_7 \geqslant 0$, and establish the relation between the number of branches of stability and the number of roots of the discriminant Δ, which depends on ρ, H, F, and K.

2.1. A geometrical formulation of the problem

The approach to be found here was inspired by the work of Ovsyannikov [21], where the problem of finding the real solutions of a quadratic equation is solved geometrically by finding the intersection points between two curves on the plane. To show this, we rewrite (2) as

$$\left[\left(1+\frac{1}{3}H^2K^2\right)p^2-1\right]\left[\left(1+\frac{1}{3}K^2\right)q^2-1\right] + \rho\left[H^2K^2\left(1+\frac{1}{12}H^2K^2\right)p^4-1\right]=0, \tag{5}$$

by defining

$$c - U_1 = q\sqrt{gH_1}, \quad c - U_2 = p\sqrt{gH_2}. \tag{6}$$

As a consequence of (6), it can be noticed that p and q are related by

$$q = \sqrt{H}p + F, \tag{7}$$

and, therefore, finding the solutions of (2) is equivalent to finding the solutions of the system of equations for p and q given by (5) and (7).

On the (p, q)-plane, Equation (5) defines a family of fourth-order curves (with two axes of symmetry) depending on ρ, H, and K. On the other hand, the slope and the initial ordinate of the straight line (7) are specified with H and F, respectively. Then, each intersection point between the fourth-order curves and the straight line represents a real solution of the system given by Equations (5) and (7).

This geometrical representation illustrates clearly how the number of real solutions varies with increasing values of F and, more importantly, shows that the system has at least two and at most four real solutions (see Figure 2). As a result, we can reduce the set of conditions in Theorem 1 to $\Delta \geqslant 0$.

The case of $\Delta = 0$ separating the two scenarios (two or four real solutions) corresponds to the special case for which the straight line described by (7) becomes tangent to the curve (5) (see [9]).

For fixed ρ and H, the determinant Δ can be written as a fifth-degree polynomial function of F^2 whose coefficients depend on K. Then, the number

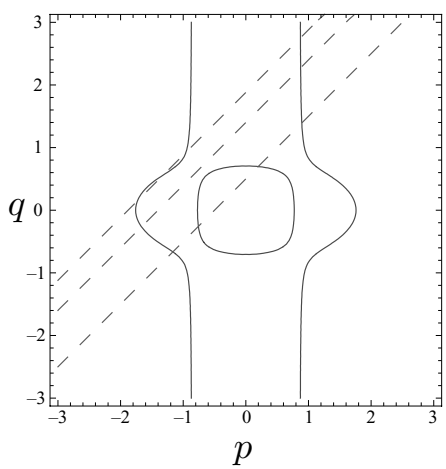

Figure 2. Solutions of the system given by Equations (5) and (7) represented by the intersection points between fourth-order curves (solid lines) and straight lines (dashed lines) for fixed values of $\rho = 1/3$, $H = 1$, and $K = 1$. Different straight lines correspond to different values of the Froude number F and lead to a different number of solutions of the system.

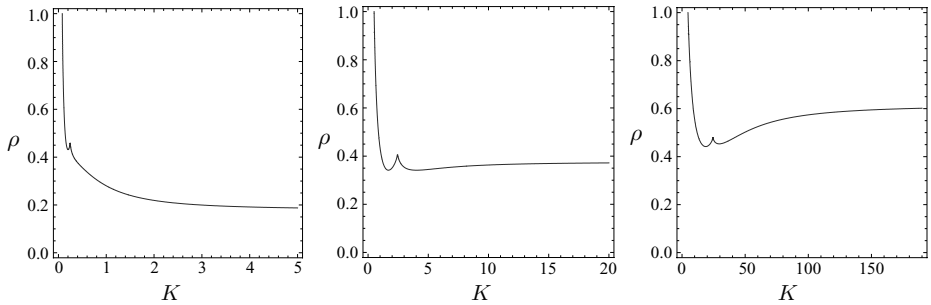

Figure 3. Curve separating the regions of one or three real roots of Δ for three different values of H (from the left to the right, we have set $H = 10$, $H = 1$, and $H = 1/10$). Inside of the region on the (K, ρ)-plane below the curve, Δ has three real roots. Otherwise, Δ has a single real root. This explains the distinction between the cases presented in Figure 1. It is worth noting that more intricate cases are found for intermediate density ratios.

of positive real roots of Δ is important since it determines the number of branches of stability on the (F, K)-plane. More precisely, *two* cases have to be considered:[2] (a) one real root for Δ and consequently one single branch of stability; (b) three real roots for Δ and, consequently, two branches of stability on the (F, K)-plane. Notice that $\Delta = 0$ represents the boundaries between the stable and unstable regions in Figure 1 and a line of $K =$ constant can intersect with the boundaries once or three times depending on the magnitude of K. Without going into detail, we just point out that it is possible to analytically distinguish the two listed cases and to display, for any fixed value of H, the regions on the (K, ρ)-plane corresponding to each one of these two cases, as shown in Figure 3.

2.2. Kelvin–Hemlholtz instability

We will now prove that the time-dependent strongly nonlinear model suffers from the KH instability by showing that F tends to zero as K approaches to ∞ along the neutral stability curve defined by $\Delta = 0$. Then, we can conclude that, for any nonzero shear (even if arbitrarily small) between layers, there exists a critical wave number beyond which the dispersion relation given by (4) has complex solutions.

To study this limit, it is convenient to consider Δ as a polynomial on the variable K. Let b_0 be the highest-order coefficient of this polynomial (with degree 26). Along the neutral stability curve of $\Delta = 0$, the limit as $K \to \infty$

[2]In general, the quintic equation $\Delta = 0$ could have five positive real roots, but this case is ruled out by the geometrical representation of the problem, since this would imply the existence of five tangency points between the straight line (7) and the curve (5), which is impossible.

leads to $b_0 = 0$. Since b_0 is given by

$$b_0 = -147456\,\rho\,(4 + 3\rho H)H^{14}F^{10},$$

we conclude that this can happen only if $F = 0$, and so the result follows.

Whenever the interface is displaced from its equilibrium position, a jump in tangential velocity is induced in the strongly nonlinear model. Therefore, the model becomes ill-posed and not suited for the numerical study of the dynamics of large amplitude internal solitary waves. To overcome this difficulty, we will adopt the idea of Choi et al. [17] for the rigid-lid model and derive a regularized free-surface model that inhibits this KH instability.

3. Derivation of a regularized model

In this section, we will derive a new strongly nonlinear model that is asymptotically equivalent to the original model (1), but has a different dispersive behavior for short waves. The strategy presented here is similar to the one found in [17], where the depth-averaged velocities $\bar{u}_i$ in the original equations are replaced by $\hat{u}_i$, the velocities evaluated at certain vertical levels $\hat{z}_i$, neglecting all the terms of $O(\varepsilon^4)$ or higher, where ε is the small parameter representing the ratio of a typical vertical scale to a typical horizontal scale. First, we will show how the velocities $\bar{u}_i$ and $\hat{u}_i$ are related. Then, using this relationship, we will propose a new model to describe large amplitude internal solitary waves and, by means of local stability analysis, show that the KH instability can indeed be suppressed up to a certain critical shear between layers.

3.1. Relationship between the depth-averaged velocities and the horizontal velocities at particular depth levels

We first consider the mass conservation laws in nondimensional variables:

$$u_{ix} + w_{iz} = 0, \tag{8}$$

where the vertical coordinate z is measured upward from the flat bottom. We assume, accordingly to Choi and Camassa [10], that the components $f = (u_i, w_i)$ of the vector velocity can be asymptotically expanded as

$$f(x, z, t) = f^{(0)} + \varepsilon^2 f^{(1)} + O(\varepsilon^4).$$

Set $i = 1$ and integrate (8), using the boundary condition $w_1(x, z = 0, t) = 0$, to obtain

$$w_1 = -z\,u_{1x}^{(0)} - \varepsilon^2 \int_0^z u_{1x}^{(1)}\,\mathrm{d}z + O(\varepsilon^4).$$

It follows that the leading order of the vertical velocity is given by

$$w_1^{(0)} = -z\, u_{1x}^{(0)}.$$

Assuming that the flow is irrotational so that

$$u_{iz} = \varepsilon^2 w_{ix},$$

or equivalently

$$u_{1z}^{(1)} = w_{1x}^{(0)},$$

leads to the relation

$$u_{1z}^{(1)} = -z\, u_{1xx}^{(0)},$$

which can be integrated to produce

$$u_1^{(1)} = u_1\big|_{z=0} - \frac{1}{2} u_{1xx}^{(0)} z^2.$$

Combining the results, we may write

$$u_1 = u_1^{(0)} + \varepsilon^2 \left(-\frac{1}{2} u_{1xx}^{(0)} z^2 \right) + O(\varepsilon^4), \tag{9}$$

where the value of the horizontal velocity at the bottom is irrelevant here since it can be absorbed by the leading-order term (that is only a function of x and t). By the definition of the depth-averaged velocities, it follows that

$$\bar{u}_1 = u_1^{(0)} + \varepsilon^2 \left(-\frac{1}{6} u_{1xx}^{(0)} h_1^2 \right) + O(\varepsilon^4).$$

On the other hand, we can deduce from (9) that the horizontal velocity u_1 is evaluated at a particular level $0 \leqslant \hat{z}_1 \leqslant h_1(x, t)$:

$$\hat{u}_1 = u_1^{(0)} + \varepsilon^2 \left(-\frac{1}{2} u_{1xx}^{(0)} \hat{z}_1^2 \right) + O(\varepsilon^4).$$

As a result, the following relation between $\bar{u}_1$ and $\hat{u}_1$ holds:

$$\hat{u}_1 = \bar{u}_1 + \varepsilon^2 \left(-\frac{1}{2} \hat{u}_{1xx} \hat{z}_1^2 + \frac{1}{6} \hat{u}_{1xx} h_1^2 \right) + O(\varepsilon^4),$$

which we can write in dimensional variables as

$$\bar{u}_1 = \hat{u}_1 + \frac{1}{2} \hat{u}_{1xx} \hat{z}_1^2 - \frac{1}{6} \hat{u}_{1xx} h_1^2 + O(\varepsilon^4). \tag{10}$$

We proceed in a completely analogous way with the lighter fluid ($i = 2$). This time, we integrate (8) to obtain

$$w_2 = w_2\Big|_{z=h_1} - (z - h_1)\, u_{2x}^{(0)} - \varepsilon^2 \int_{h_1}^{z} u_{2x}^{(1)}\, \mathrm{d}z + O(\varepsilon^4),$$

which is precisely

$$w_2^{(0)} = -u_{2x}^{(0)}\,(z - h_1) + h_{1t} + u_2^{(0)} h_{1x},$$

when the kinematic boundary condition is imposed at the interface. Using the fact that the flow is irrotational allows us to write

$$u_{2z}^{(1)} = -u_{2xx}^{(0)}\,(z - h_1) + g(x, t),$$

with $g(x, t)$ defined by

$$g(x, t) = u_{2x}^{(0)}\, h_{1x} + \left(h_{1t} + u_2^{(0)} h_{1x}\right)_x.$$

Integrating the last relation leads to

$$u_2^{(1)} = u_2\Big|_{z=h_1} - \frac{1}{2} u_{2xx}^{(0)}\,(z - h_1)^2 + g(x, t)\,(z - h_1),$$

and, considering that the integration constant is irrelevant, as mentioned before, we may write

$$u_2 = u_2^{(0)} + \varepsilon^2 \left(-\frac{1}{2} u_{2xx}^{(0)}\,(z - h_1)^2 + g(x, t)\,(z - h_1) \right) + O(\varepsilon^4). \tag{11}$$

By the definition of the depth-averaged velocities, we have

$$\bar{u}_2 = u_2^{(0)} + \varepsilon^2 \left(-\frac{1}{6} u_{2xx}^{(0)}\, h_2^2 + \frac{1}{2} g(x, t)\, h_2 \right) + O(\varepsilon^4).$$

On the other hand, we know from (11) that at a particular vertical level $h_1 \leqslant \hat{z}_2 \leqslant (h_1 + h_2)$, the horizontal velocity u_2 is given by

$$\hat{u}_2 = u_2^{(0)} + \varepsilon^2 \left(-\frac{1}{2} u_{2xx}^{(0)}\,(\hat{z}_2 - h_1)^2 + g(x, t)\,(\hat{z}_2 - h_1) \right) + O(\varepsilon^4),$$

and consequently

$$\begin{aligned} \hat{u}_2 = \bar{u}_2 + \varepsilon^2 \Big(& -\frac{1}{2} \hat{u}_{2xx}\,(\hat{z}_2 - h_1)^2 + \hat{g}(x, t)\,(\hat{z}_2 - h_1) \\ & + \frac{1}{6} \hat{u}_{2xx}\, h_2^2 - \frac{1}{2} \hat{g}(x, t)\, h_2 \Big) + O(\varepsilon^4), \end{aligned}$$

where we have introduced $\hat{g}(x,t)$ defined by

$$\hat{g}(x,t) = \hat{u}_{2x}\, h_{1x} + (h_{1t} + \hat{u}_2 h_{1x})_x\,.$$

This establishes the desired relation between $\bar{u}_2$ and $\hat{u}_2$:

$$\bar{u}_2 = \hat{u}_2 + \frac{1}{2}\hat{u}_{2xx}\,(\hat{z}_2 - h_1)^2 - \frac{1}{6}\hat{u}_{2xx}\, h_2^2 - \hat{g}(x,t)\,(\hat{z}_2 - h_1) + \frac{1}{2}\hat{g}(x,t)\, h_2 + O(\varepsilon^4). \tag{12}$$

We point out that we have not used here the fact that $\hat{z}_i =$ constant. Nothing prevents us from considering $\hat{z}_i = \hat{z}_i(x,t)$, and, therefore, any vertical level $\hat{z}_i$ including $z = 0$, $z = h_1(x,t)$ or $z = (h_1 + h_2)(x,t)$ can be chosen, whenever applicable.

3.2. Derivation of an asymptotically equivalent model with an improved dispersion relation

We go back to (1) and substitute the expressions (10) and (12) for $\bar{u}_1$ and $\bar{u}_2$. Neglecting all the terms of $O(\varepsilon^4)$ or higher will provide a new system of nonlinear evolution equations for h_i and $\hat{u}_i$. We start with the mass conservation law for the heavier fluid that leads to

$$h_{1t} + \left[h_1\left(\hat{u}_1 + \frac{1}{2}\hat{z}_1^2\,\hat{u}_{1xx} - \frac{1}{6}h_1^2\,\hat{u}_{1xx}\right)\right]_x = 0. \tag{13}$$

Considering the mass conservation law for the lighter fluid demands care. Substituting (12) straightforwardly into the second equation in (1) includes indirectly some higher-order terms since the expression of $\hat{g}(x,t)$ contains the term h_{1t} that can be expressed from (13) as

$$h_{1t} = -(h_1\hat{u}_1)_x + O(\varepsilon^2). \tag{14}$$

To preserve asymptotic consistency in the way chosen to perturb the dispersive behavior for short waves, we should write for the lighter fluid

$$h_{2t} + \left[h_2\left(\hat{u}_2 + \frac{1}{2}(\hat{z}_2 - h_1)^2\,\hat{u}_{2xx} - \frac{1}{6}h_2^2\,\hat{u}_{2xx} - \hat{f}(x,t)(\hat{z}_2 - h_1) + \frac{1}{2}\hat{f}(x,t)h_2\right)\right]_x = 0, \tag{15}$$

with $\hat{f}(x,t)$ given by

$$\hat{f}(x,t) = \hat{u}_{2x}\, h_{1x} + [[h_1(\hat{u}_2 - \hat{u}_1)]_x - h_1\hat{u}_{2x}]_x.$$

Similarly, the momentum equation for the heavier fluid yields

$$\hat{u}_{1t} + \hat{u}_1\hat{u}_{1x} + g(h_1 + \rho h_2)_x = \left[\frac{1}{2}h_1^2\,\hat{G}_1 + \rho\left(\frac{1}{2}h_2^2\,\hat{G}_2 - \left(D_2^{\hat{2}}h_1\right)h_2\right)\right]_x - \frac{1}{2}\hat{z}_1^2\,(\hat{u}_{1xt} + \hat{u}_1\hat{u}_{1xx})_x - (\hat{z}_{1t} + \hat{u}_1\hat{z}_{1x})\hat{z}_1\hat{u}_{1xx}, \tag{16}$$

where the terms $\hat{G}_i$ and $(D_2^{\hat{2}}h_1)$ are defined as follows:

$$\hat{G}_i = \hat{u}_{ixt} + \hat{u}_i\hat{u}_{ixx} - \hat{u}_{ix}^2,$$
$$\left(D_2^{\hat{2}}h_1\right) = [-(h_1\hat{u}_1)_x(\hat{u}_2 - \hat{u}_1) + h_1(\hat{u}_2 - \hat{u}_1)_t]_x + \hat{u}_2\,[h_1(\hat{u}_2 - \hat{u}_1)]_{xx} + (h_1\hat{u}_1)_x\hat{u}_{2x} - h_1\hat{u}_{2xt} - \hat{u}_2(h_1\hat{u}_{2x})_x.$$

Finally, taking into account all the considerations made above, we have for the lighter fluid the following equation:

$$\begin{aligned}
&\hat{u}_{2t} + \hat{u}_2\,\hat{u}_{2x} + g(h_1 + h_2)_x + \frac{1}{2}(\hat{z}_2 - h_1)^2(\hat{u}_{2xt} + \hat{u}_2\,\hat{u}_{2xx})_x \\
&\quad + [\hat{z}_{2t} + \hat{u}_2\hat{z}_{2x} - [h_1(\hat{u}_2 - \hat{u}_1)]_x + h_1\hat{u}_{2x}](\hat{z}_2 - h_1)\hat{u}_{2xx} \\
&\quad + \left(-(\hat{z}_2 - h_1) + \frac{1}{2}h_2\right)\hat{F}(x,t) - \left[\hat{z}_{2t} + \left(h_1\hat{u}_1 + \frac{1}{2}h_2\hat{u}_2\right)_x\right]\hat{f}(x,t) \\
&\quad + \left[\hat{u}_2\left(-\hat{f}(x,t)(\hat{z}_2 - h_1) + \frac{1}{2}\hat{f}(x,t)h_2\right)\right]_x = \left(\frac{1}{2}h_2^2\hat{G}_2\right)_x - \left(D_2^{\hat{2}}h_1\right)h_{2x} \\
&\quad - \frac{1}{2}h_2\left(D_2^{\hat{2}}h_1\right)_x + \left(\frac{1}{2}h_2\hat{G}_2 - \left(D_2^{\hat{2}}h_1\right)\right)h_{1x},
\end{aligned} \tag{17}$$

where $\hat{F}(x,t)$ is precisely the partial time derivative $\hat{f}_t(x,t)$ written, by considering (14), as:

$$\hat{F}(x,t) = \hat{u}_{2xt}h_{1x} - \hat{u}_{2x}(h_1\hat{u}_1)_{xx} + [-(h_1\hat{u}_1)_x(\hat{u}_2 - \hat{u}_1) + h_1(\hat{u}_2 - \hat{u}_1)_t]_{xx} - [-(h_1\hat{u}_1)_x\hat{u}_{2x} + h_1\hat{u}_{2xt}]_x\,.$$

3.3. Local stability analysis

Using local stability analysis, we will investigate how the vertical levels in the new model formed by Equations (13) and (15)–(17) should be chosen to inhibit the shear instability induced by internal solitary waves. By substituting into these equations $h_i = H_i + h_i'$ and $\hat{u}_i = U_i + \hat{u}_i'$ and assuming the prime variables are small, the system linearized about $u_i = U_i$ and $h_i = H_i$ is given, after dropping the primes, by

$$h_{1t} + U_1h_{1x} + H_1\hat{u}_{1x} + \alpha_1H_1^3\,\hat{u}_{1xxx} = 0, \tag{18}$$

$$h_{2t} + U_2 h_{2x} + H_2 \hat{u}_{2x} + \alpha_2 H_2^3 \hat{u}_{2xxx} + \left(\frac{1}{2} - \theta_2\right) H_2^2 \left[(U_2 - U_1) h_{1xxx} - H_1 \hat{u}_{1xxx}\right] = 0, \tag{19}$$

$$\begin{aligned}\hat{u}_{1t} + U_1 \hat{u}_{1x} + g(h_1 + \rho h_2)_x &+ \left[\left(\alpha_1 - \frac{1}{3}\right) H_1^2 - \rho H_1 H_2\right] \hat{u}_{1xxt} \\ &+ \left[U_1 \left(\alpha_1 - \frac{1}{3}\right) H_1^2 + \rho H_1 H_2 (U_1 - 2U_2)\right] \hat{u}_{1xxx} \\ &- \frac{1}{2} \rho H_2^2 (\hat{u}_{2xxt} + U_2 \hat{u}_{2xxx}) \\ &+ \rho H_2 (U_2 - U_1)^2 h_{1xxx} = 0,\end{aligned} \tag{20}$$

$$\begin{aligned}\hat{u}_{2t} + U_2 \hat{u}_{2x} + g(h_1 + h_2)_x &+ \left(\alpha_2 - \frac{1}{3}\right) H_2^2 (\hat{u}_{2xxt} + U_2 \hat{u}_{2xxx}) \\ &+ H_2 \left(\theta_2 - \frac{1}{2}\right) [H_1 (U_2 - U_1) \hat{u}_{1xxx} + U_1 (U_2 - U_1) h_{1xxx} \\ &+ H_1 \hat{u}_{1xxt}] - H_2 U_2 \left(\theta_2 - \frac{1}{2}\right) [(U_2 - U_1) h_{1xxx} - H_1 \hat{u}_{1xxx}] \\ &+ \frac{1}{2} H_2 [(U_2 - U_1)^2 h_{1xxx} + H_1 (U_1 - 2U_2) \hat{u}_{1xxx} - H_1 \hat{u}_{1xxt}] = 0,\end{aligned} \tag{21}$$

where we have introduced

$$\theta_1 = \frac{\hat{z}_1}{H_1}, \quad \theta_2 = \frac{\hat{z}_2 - H_1}{H_2}, \quad \alpha_1 = \frac{1}{2}\theta_1^2 - \frac{1}{6}, \quad \alpha_2 = \frac{1}{2}\theta_2^2 - \frac{1}{6}.$$

By definition, $0 \le \theta_i \le 1$ and, for example, both θ_1 and θ_2 are zero when $\hat{z}_1 = 0$ and $\hat{z}_2 = H_1$, that corresponds to prescribing the vertical levels at the bottom and the interface, respectively. It is worth to note that, in contrast with the rigid-lid case [17], there are no preferred levels for which the linear dispersion relation obtained for the original strongly nonlinear model (written in terms of the depth averaged velocities) is recovered.

By looking for solutions $(h_1, h_2, \hat{u}_1, \hat{u}_2) \sim \exp[i(kx - \omega t)]$ of the linearized system formed by Equations (18)–(21), we obtain the linear dispersion relation between ω and k. An important consideration in choosing the vertical levels θ_1 and θ_2 is that the wave speed must be real for all k, at least, in the absence of background shear.

3.3.1. *Linear dispersion relation in the absence of shear.* Setting $U_1 = U_2 = 0$ leads to the following dispersion relation in dimensionless form:

$$A\,\bar{c}^4 + B\,\bar{c}^2 + C = 0, \tag{22}$$

where $\bar{c}$ is the nondimensional wave speed defined in (3) and the coefficients are given by

$$\begin{aligned}
A &= 36 + 18\big[\big(1-\theta_1^2\big) + H^2\big(1-\theta_2^2\big) + 2\rho H\big]K^2 \\
&\quad + 9H^2(1-\theta_2)\big[(\theta_2+1)\big(1-\theta_1^2\big) + 2\rho H\theta_1\big]K^4, \\
B &= -36(1+H) + 6(1+H)\big[3\theta_1^2 - 1 - 2H + \big(3\theta_1^2-1\big)H^2\big]K^2 \\
&\quad + 3H^2\big[-H\big(\theta_1^2-1\big)\big(3\theta_2^2-1\big) \\
&\quad + \rho H^2\theta_2(3\theta_2-2) - \big(3\theta_1^2-1\big)\big(-1+\theta_2^2+\rho\big)\big]K^4, \\
C &= (1-\rho)H\big[-6 + K^2\big(3\theta_1^2-1\big)\big]\big[-6 + H^2K^2\big(3\theta_2^2-1\big)\big].
\end{aligned}$$

It is clear that $A > 0$ for any parameter values. As a consequence, there are four distinct real roots of (22) if all of the following conditions are satisfied: (i) $B^2 - 4AC > 0$; (ii) $B < 0$; (iii) $C > 0$. In particular, from the condition $C > 0$, it follows that $0 \le \theta_i^2 \le 1/3$. This shows, for example, that the cases when the vertical levels are chosen at the interface and the free surface ($\theta_1 = \theta_2 = 1$), or at the bottom and the free surface ($\theta_1 = 0$ and $\theta_2 = 1$), have to be excluded. We would think, based on the rigid-lid case, that the natural choice here would be prescribing the vertical levels at the bottom and top boundaries [17], but, as we have shown, this cannot be the case.

Even though the dispersion relation (22) is a bi-quadratic form, it is quite challenging to find the ranges of θ_1 and θ_2 for which the problem is well-posed for any physical parameters. Our numerical tests show that the first stability condition (i) reduces drastically the number of possible choices for these parameters. To simplify our task, we first seek the vertical levels θ_1 and θ_2 that satisfy $B^2 - 4AC > 0$ for any physical parameters ρ and H in the limit of $K \to \infty$ and, then, confirm the result for arbitrary K.

When considering the limit $K \to \infty$, our numerical search over the (θ_1, θ_2)-plane rules out any pair of values (θ_1, θ_2) in the interior of the square $(0, \sqrt{3}/3) \times (0, \sqrt{3}/3)$. Additionally, it can be shown that the line segments given by $\theta_1 = 0$ (with the exception of the origin) and $\theta_2 = \sqrt{3}/3$ have to be excluded for stability in the absence of a velocity jump. This leaves us as remaining candidates the line segments $\theta_2 = 0$ and $\theta_1 = \sqrt{3}/3$.

To test these candidates, we consider now an arbitrary K. We observe that, along each one of these line segments, the only stability criterion not trivially satisfied is condition (i). However, it can be shown numerically that $B^2 - 4AC$ is a concave upward parabola with no positive real roots for ρ, for any given H and K. As a conclusion, the new nonlinear system is stable in the absence of background shear for any pair of values (θ_1, θ_2) on the line segments $\theta_2 = 0$ or $\theta_1 = \sqrt{3}/3$.

3.3.2. *A regularized model in the presence of shear.* Our next step could be to determine, through local stability analysis, θ_1 and θ_2 that have the greatest

inhibiting effect upon the KH instability in the presence of shear ($U_1 \neq U_2$, or $F \neq 0$). However, keeping in mind the complexity of the proposed model, another important consideration regarding the choice of these values is finding the model in its simplest form, more suited for analytical and numerical studies. From Equations (13) and (15)–(17), it is quite obvious that this is attained when both θ_1 and θ_2 are zero, which corresponds to prescribing the vertical levels at the bottom and interface, respectively. This choice might not inhibit the KH instability for the largest range of Froude number F, but it would be an optimum choice for numerical computations. Indeed, in this case, the system formed by Equations (13) and (15)–(17) simplifies dramatically to:

$$h_{1t} + \left[h_1 \left(\hat{u}_1 - \frac{1}{6} h_1^2 \, \hat{u}_{1xx} \right) \right]_x = 0, \tag{23}$$

$$h_{2t} + \left[h_2 \left(\hat{u}_2 - \frac{1}{6} h_2^2 \, \hat{u}_{2xx} + \frac{1}{2} \hat{f}(x,t) h_2 \right) \right]_x = 0, \tag{24}$$

$$\hat{u}_{1t} + \hat{u}_1 \hat{u}_{1x} + g(h_1 + \rho h_2)_x = \left[\frac{1}{2} h_1^2 \, \hat{G}_1 + \rho \left(\frac{1}{2} h_2^2 \, \hat{G}_2 - \left(D_2^{\hat{2}} h_1 \right) h_2 \right) \right]_x, \tag{25}$$

$$\begin{aligned} &\hat{u}_{2t} + \hat{u}_2 \, \hat{u}_{2x} + g(h_1 + h_2)_x + \frac{1}{2} h_2 \, \hat{F}(x,t) + \frac{1}{2} h_2 \hat{u}_2 \, \hat{f}_x(x,t) \\ &\quad = \left(\frac{1}{2} h_2^2 \hat{G}_2 \right)_x - \left(D_2^{\hat{2}} h_1 \right) h_{2x} - \frac{1}{2} h_2 \left(D_2^{\hat{2}} h_1 \right)_x + \left(\frac{1}{2} h_2 \hat{G}_2 - \left(D_2^{\hat{2}} h_1 \right) \right) h_{1x}. \end{aligned} \tag{26}$$

Its dispersion relation is, as in (4), a quartic equation in $\bar{c}$:

$$a_0 \bar{c}^4 + a_1 \bar{c}^3 + a_2 \bar{c}^2 + a_3 \bar{c} + a_4 = 0, \tag{27}$$

where the coefficients have now new expressions.[3] Unfortunately, the solution behavior of Equation (27) is much more complicated than that of Equation (4). For example, for the new system, it is not clear if the conditions given by Theorem 1 can be reduced to $\Delta \geqslant 0$, which is the case for the original system. A geometrical interpretation presented in §2.1 for the original model could be adopted, but does not bring any new insight into the problem since the corresponding fourth-order curves on the (p, q)-plane will depend not only on ρ, H, K, but also on F. Nevertheless, our numerical tests indicate that this reduction holds also here.

[3]The expressions for these coefficients are too long to be presented here.

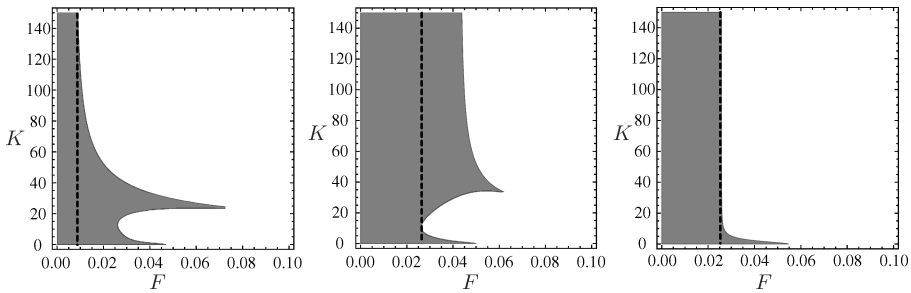

Figure 4. Shear instability of the model given by Equations (23)–(26) with $\rho = 0.998$ on the (F, K)-plane for three different depth ratios: $H = 1/10$, $H = 1/4$, and $H = 1/2$. Here, the shaded and unshaded regions represent the stable and unstable regions, respectively. The dashed vertical lines represent the critical Froude number F_{cr} for each case. We remark that in each one of these cases, only the first branch of stability is considered.

Because the highest-order coefficient a_0 of Equation (27) is found to be still positive for any given parameters, we still can apply Theorem 1 to visualize numerically the stable and unstable regions on the (F, K)-plane for fixed ρ and H (*cf.* Figure 4). To demonstrate that the KH instability is contained in the new model, we choose a density ratio $\rho = 0.998$ that is relevant for oceanic applications.

The critical Froude number F_{cr} denoted by dashed lines in Figure 4 is defined as the minimum Froude number below which the system is stable for all K. Depending on H, the critical Froude number is determined by either a vertical asymptote, say F_A, as $K \to \infty$ or a vertical tangent to the curve of $\Delta = 0$ defined by $\Delta\ (F, K) = \partial_K\ \Delta\ (F, K) = 0$.[4]

Figure 5 shows the critical Froude number F_{cr} for varying H for both the rigid-lid and free-surface configurations. For the rigid-lid configuration, the regularized system is found to be linearly stable if $F \leqslant \frac{\sqrt{3}}{3} F_0^{\mathrm{rigid}}$, where F_0^{rigid} represents the critical Froude number obtained in the long-wave limit as $K = 0$ (see [17]). For the free-surface configuration, we have, in the long-wave limit, two critical Froude numbers F_0^- and F_0^+. For density ratios close to 1, $F_0^- \approx F_0^{\mathrm{rigid}}$. For example, for $\rho = 0.998$ and $H = 0.2$, we have $F_0^- \approx 0.048997$ and $F_0^{\mathrm{rigid}} \approx 0.048998$. The regularized model for the rigid-lid configuration is stable for $F \leqslant 0.0283$ while the new regularized model for the free-surface case is stable for $F \leqslant F_{\mathrm{cr}}$ with $F_{\mathrm{cr}} \approx 0.0263$. For other values of H, the critical Froude number for the free-surface model is found to be always smaller than that for the regularized rigid-lid model. We stress that the original

[4]This statement also holds for different density ratios.

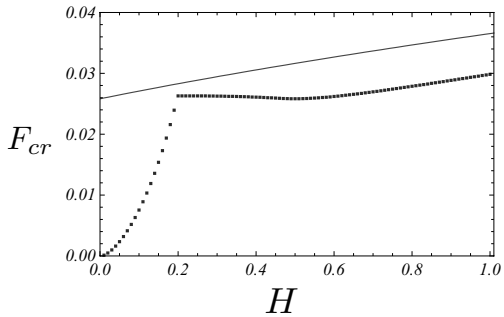

Figure 5. Critical Froude number F_{cr} versus depth ratio H for $\rho = 0.998$: The free surface model (dotted line) and the rigid-lid model (solid line). For the free-surface case (dotted line) the curve is continuous but not regular at the transition points between the two possible scenarios for the critical Froude number (vertical asymptote or vertical tangent) (*cf.* Figure 4).

model is always unstable, which means its critical Froude number is zero. Therefore, the new system given by (23)–(26) is indeed regularized for a wide range of depth ratios relevant for real applications.

4. Concluding remarks

Motivated by the fact that the strongly nonlinear model for a two-layer system (1) written in terms of the depth-averaged velocities suffers from the KH instability, we derived a new model written in terms of the horizontal velocities at the bottom and the interface. The two systems are asymptotically equivalent for long waves, but the dispersive behaviors of short waves are different. Through local stability analysis, the new system is found regularized and the KH instability is contained as long as the shear between the two layers does not exceed a certain critical Froude number.

It was shown that other vertical levels could have been considered. The choice of $\theta_1 = \theta_2 = 0$ was made mainly by the simplicity requirement for the model; hence, this might not be the best possible choice regarding the greatest inhibiting effect upon the KH instability. Nonetheless, the new regularized model can serve as an effective mathematical model for large amplitude internal waves propagating under the effect of the top free surface.

No numerical evidence supporting the result from local stability analysis is presented in this paper, but, based on our previous experience with the regularized rigid-lid model [17], the new model will be of value for future numerical investigation. Considering the richness of solitary wave solutions of the original free surface model, it is of interest to study numerically the dynamics of such waves using the regularized free surface model for a wide

range of physical parameters, including front wave solutions of the maximum wave amplitude.

For the rigid-lid case, the Froude number induced by a solitary wave at the maximal interfacial displacement can be related analytically to the wave amplitude. Therefore, it can be stated that, when the regularized strongly nonlinear model is used, internal solitary waves are stable to perturbations of arbitrary wavelengths if the wave amplitudes are smaller than a critical value. It would be interesting to obtain an analogous result for the free surface case, but no analytic relationship between the Froude number and the wave amplitude has been found yet.

Acknowledgments

The authors gratefully acknowledge support from NSF through Grant DMS-0620832 and ONR through Grant N00014-08-1-0377.

Appendix A: Linear Dispersion for the Original Strongly Nonlinear Model

The linear dispersion relation for the original model (1) is found in dimensionless form as:

$$a_0\bar{c}^4 + a_1\bar{c}^3 + a_2\bar{c}^2 + a_3\bar{c} + a_4 = 0,$$

where the expressions for the coefficients are the following:

$$\begin{aligned}
a_0 &= (3\rho H + 4)H^2K^4 + 12(H^2 + 3\rho H + 1)K^2 + 36,\\
a_1 &= -12(F+1)H(H^2K^2 + 12)\rho K^2 - 8(F+2)(K^2+3)(H^2K^2+3),\\
a_2 &= 2[(H^2(9H\rho + 2)K^4 + 6(H^2 + 18\rho H + 1)K^2 + 18)F^2\\
&\quad + 6[H^2(3H\rho + 2)K^4 + 6(H^2 + 6\rho H + 1)K^2 + 18]F\\
&\qquad - 18(-2K^2 + H - 5) + 3HK^2(36\rho + H((3H\rho + 4)K^2 + 10) - 2)],\\
a_3 &= -12HK^2(H^2K^2 + 12)\rho(F+1)^3 - 8[(K^2+3)(H^2K^2+3)F^2\\
&\quad + 3(K^2+2)(H^2K^2+3)F + 6K^2 + H(2HK^4 + 3(H-1)K^2 - 9) + 9],\\
a_4 &= (F+1)^2H^2(3H\rho(F+1)^2 + 4)K^4 + 12(3H\rho(F+1)^4\\
&\quad + F^2 + 2F - H + 1)K^2 - 36\rho H.
\end{aligned}$$

Appendix B: Stability Behavior of the New Regularized System for High Wavenumbers

By considering the limit of $K \to \infty$ along the neutral stability curve given by $\Delta = 0$, we are able to find vertical asymptotes $F = F_A$, as described in Section 3.3.2, as roots of the highest-order coefficient of Δ as a polynomial in the variable K. This time, these roots are found as roots of a fifth-degree

polynomial P in the variable $y = F^2$:

$$P(y) = d_0\, y^5 + d_1\, y^4 + d_2\, y^3 + d_3\, y^2 + d_4\, y + d_5,$$

whose coefficients are given below:

$$\begin{aligned}
d_0 &= 96\,\rho\,(3H + 2\rho)^3,\\
d_1 &= -8[162(2\rho + 1)H^4 + 108(7 - 9\rho)\rho H^3 + 9\rho^2(13\rho + 96)H^2\\
&\quad + 12(28 - 27\rho)\rho^3 H + 4(8 - 11\rho)\rho^4],\\
d_2 &= 4H[164\rho^5 - 2(79H + 146)\rho^4 + 4(H(279H - 190) + 32)\rho^3\\
&\quad - 9H(H(155H + 59) - 80)\rho^2 + 108(H - 5)(H - 2)H^2\rho\\
&\quad + 432H^3(H + 1)],\\
d_3 &= H^2[48(7\rho - 18)H^4 - 72(\rho(23\rho - 64) + 8)H^3 + 12(\rho(\rho(167\rho - 364)\\
&\quad + 140) - 72)H^2 + \rho(\rho((644 - 505\rho)\rho + 1352) - 1248)H\\
&\quad + 24(\rho - 1)^2\rho^2(19\rho - 16)],\\
d_4 &= -4H^3[12(3\rho - 4)H^4 + ((148 - 193\rho)\rho + 48)H^3 - (\rho - 1)(49(\rho - 4)\rho\\
&\quad + 48)H^2 - (\rho - 1)^2(\rho(47\rho + 4) + 48)H - (\rho - 1)^3\rho(35\rho - 32)],\\
d_5 &= 16H^4(\rho - 1)(H + \rho - 1)^4.
\end{aligned}$$

This quintic equation has one, three, or five nonnegative real roots ${F_A}^2$, depending on the parameters considered (see Figure B1). Notice that, even

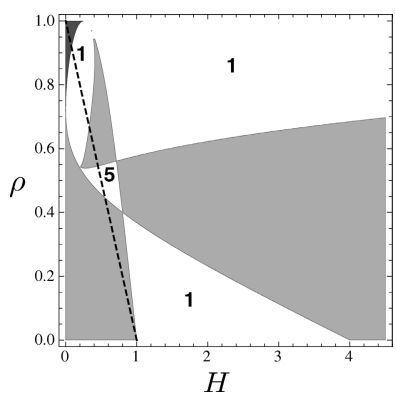

Figure B1. Number of real roots of the polynomial P through the $(H,\ \rho)$-plane. In the dashed region, P has three real solutions. Otherwise, P has one or five real roots, as specified in the figure. Bearing in mind that $y = F^2$, it is essential to guarantee that these roots are all nonnegative. It can be proven that this is true everywhere, except for the darker shaded region on the upper-left corner, where despite of having three real roots, only one is nonnegative. In this figure, the dashed line is defined by $H = 1 - \rho$ and corresponds to the exceptional case when $P(0) = 0$.

if these values do not have to lead to the critical Froude number F_{cr} (see Figure 4), these are still candidates for F_{cr}.

Additionally, given fixed parameter values ρ and H, if all the roots F_A are positive, this implies that the new derived model is able to contain the KH instability up to a certain critical Froude number $F_{\mathrm{cr}} > 0$, less or equal to the minimum of these roots F_A.

Finally, we remark that this feature cannot be achieved for every parameter values since, for $H = 1 - \rho$, we have $d_5 = 0$ or, equivalently, $P(0) = 0$.

References

1. M. Miyata, Long internal waves of large amplitude, in *Proceedings of the IUTAM Symposium on Nonlinear Water Waves* (H. Horikawa and H. Maruo, Eds.), pp. 399–406, 1988.
2. W. Choi and R. Camassa, Fully nonlinear internal waves in a two-fluid system, *J. Fluid Mech.* 396:1–36 (1999).
3. R. Camassa, W. Choi, H. Michallet, P. Rusas, and J. K. Sveen, On the realm of validity of strongly nonlinear asymptotic approximations for internal waves, *J. Fluid Mech.* 549:1–23 (2006).
4. J. Grue, A. Jensen, P. E. Rusas, and J. K. Sveen, Properties of large-amplitude internal waves, *J. Fluid Mech.* 380:257–278 (1999).
5. H. Michallet and E. Barthélemy, Experimental study of interfacial solitary waves, *J. Fluid Mech.* 366:159–177 (1998).
6. H. Michallet and F. Dias, Numerical study of generalized interfacial solitary waves, *Phys. Fluids* 11:1502–1511 (1999).
7. F. Dias and A. Il'ichev, Interfacial waves with free-surface boundary conditions: An approach via a model equation, *Phys. D* 150:278–300 (2001).
8. R. Barros and S. L. Gavrilyuk, Dispersive nonlinear waves in two-layer flows with free surface. II. Large amplitude solitary waves embedded into the continuous spectrum, *Stud. Appl. Math.* 119:213–251 (2007).
9. R. Barros and W. Choi, On the hyperbolicity of two-layer flows, in *Proceedings of the 2008 Conference on FACM'08 held at New Jersey Institute of Technology*, USA, 19–21 May 2008.
10. W. Choi and R. Camassa, Weakly nonlinear internal waves in a two-fluid system, *J. Fluid Mech.* 313:83–103 (1996).
11. R. Barros, S. L. Gavrilyuk, and V. M. Teshukov, Dispersive nonlinear waves in two-layer flows with free surface. Part I. Model derivation and general properties, *Stud. Appl. Math.* 119:191–211 (2007).
12. C. H. Su and C. S. Gardner, Korteweg-de Vries Equation and Generalizations. Part III. Derivation of the Korteweg-de Vries Equation and Burgers Equation, *J. Math. Phys.* 10:536–539 (1969).
13. A. E. Green and P. M. Naghdi, A derivation of equations for wave propagation in water of variable depth, *J. Fluid Mech.* 78:237–246 (1976).
14. R. Liska, L. Margolin, and B. Wendroff, Nonhydrostatic two-layer models of incompressible flow, *Comput. Math. Appl.* 29:25–37 (1995).

15. T.-C. Jo and W. Choi, Dynamics of strongly nonlinear solitary waves in shallow water, *Stud. Appl. Math.* 109:205–227 (2002).
16. T.-C. Jo and W. Choi, On stabilizing the strongly nonlinear internal wave model, *Stud. Appl. Math.* 120:65–85 (2008).
17. W. Choi, R. Barros, and T.-C. Jo, A regularized model for strongly nonlinear internal solitary waves, *J. Fluid Mech.* (2008), in press.
18. H. Y. Nguyen and F. Dias, A Boussinesq system for two-way propagation of interfacial waves, *Phys. D* 237:2365–2389 (2009).
19. E. I. Jury and M. Mansour, Positivity and nonnegativity conditions of a quartic equation and related problems, *IEEE Trans. Automat. Contr.* AC-26:444–451 (1981).
20. A. T. Fuller, Root location criteria for quartic equations, *IEEE Trans. Automat. Contr.* AC-26:777–782 (1981).
21. L. V. Ovsyannikov, Two-layer "shallow water" model, *J. Appl. Mech. Tech. Phys.* 20:127–135 (1979).

New Jersey Institute of Technology

(Received December 10, 2008)